Volume 9, Number 12
1009-1963/2000/09(12)/0892-08
CHINESE PHYSICS
December, 2000
© 2000 Chin. Phys. Soc.

ASYMMETRY PARAMETERS AND DIFFERENTIAL CROSS SECTIONS FOR PHOTOIONIZATION-EXCITATION OF HELIUM*

Jiang Yu-hai(江玉海), Sun Jin-feng(孙金锋),
Zhu Zun-lue(朱遵略), Yang Qin-yu(杨沁玉), Wan Ling-de(万陵德)
College of Physics and Information Engineering, Henan Normal University, Xinxiang 453002, *China*

(Received 7 April 2000)

Asymmetry parameter β_2 for photoionization of helium leaving the He^+ ion in the $n = 2$ level and differential cross sections(DCSs) in the $n = 2, 3, 4$ levels with photon emission angle $\theta = 90^0$ are provided at photon energies $69 - 76.8$ eV employing the R-matrix method with a 20-term target representation, in which five polarization orbitals $\bar{6}l$ are included. The asymmetry parameter β_2 and the DCS, in the $n = 2$ level in the region of $69 - 73$ eV, are in good agreement with available experimental and theoretical results. Above the $n = 3$ threshold, we present new theoretical results along with measurements. No theoretical and experimental results can be used to compare with the present calculations of the DCSs for photoionization into the He^+ ion in the $n = 3, 4$ levels.

Keywords: Asymmetry parameter, differential cross sections, photoionization, R-matrix
PACC: 3400

I. INTRODUCTION

The photoionization-excitation cross sections of helium leaving $He^+(n)$ ion in excited states, which are related to radiative-recombination transitions in plasmas, play an important role in opacity project. And helium is also an example in a two-electron system to study electron correlation effects. The fact that direct photon ionization and autoionization from highly correlated doubly excited states can interfere makes these studies a challenging task for theoreticians, particularly in the evaluation of partial cross sections for different $He^+(n)$ ion levels. In the past 20 years, a lot of experimental[1−4] and theoretical[5−12] efforts have been focused on the calculation of total cross sections and resonance properties of photoionization on helium leaving He^+ ion in an excited state. In this article, we are concerned with the asymmetry parameters β and the partial differential cross sections (DCSs) for photoionization of helium from $n = 2$ to $n = 5$ thresholds ($69 - 76.8$ eV). The asymmetry parameters β and DCSs for photoionization, which contain information of the dynamics of the photoionization process, are much more sensitive to small deficiencies in the wave functions than the total cross sections. The shapes of β and DCSs for photoionization are slightly more complex and depend on the ionization channels considered. Therefore, the β and DCSs can be used as more stringent tests of various methods than total cross sections for photoionization. An experimental determination of β_2 for photoionization into the $He^+(n{=}2)$ states was carried out by Lindle *et al.*[13] Recently, the β_2 and the DCSs for photoionization into the He^+ $(n = 2)$ state at 90° angle have been studied in experiment by Zubek *et al.*[14] with linearly polarized light over the photon energies $69 - 77$ eV, where photoionization is dominated by abundant autoionization states from doubly-excited states of helium, and no measurements for $He^+(n = 3, 4)$ states are found up to now in the present region concerned. Sanchez and Martin[7] in 1992 reported their theoretical results of the differential cross section $d\sigma_{n=2}/d\Omega$ of photoionization at $\theta = 90°$ angle and asymmetry parameter β_2 at incident photon energies $69 - 73$ eV (between the $n = 2$ and $n = 3$ thresholds of the He^+ ion) by the use of a Feshbach partitioning of final-state wave function and an L^2 representation of the coupled continuum states. No other results of β_2 and DCSs for photoionization into the He^+ $(n = 2, 3, 4)$ ion states at $\theta = 90°$ are found above photon energy 73 eV in the literature. In the present paper, we employ the R-matrix approach[15,16] to calculate the β_2 and the DCSs for photoionization of helium leaving the He^+ in $n = 2, 3, 4$ states at $\theta = 90°$ below the $n = 5$ threshold of He^+ ion. Atomic units and energy in Rydberg are used throughout this paper if not specified.

II. R-MATRIX OF PHOTOIONIZATION

In this paper, partial cross sections for photoion-

*Project supported by the Natural Science and Theoretical Education Foundation of Henan Province, China (1999140009).

ization are calculated for the following process

$$h\nu + \mathrm{He}(1s^2)\ \ ^1S \rightarrow [\mathrm{He}^+(nl) + e(n'l')]\ \ ^1P^o. \quad (1)$$

For the case of photoionization ejected from unpolarized target atoms by linear polarized radiation, the differential cross sections $\mathrm{d}\sigma(L_iS_i \rightarrow L_fS_f)/\mathrm{d}\hat{k_f}$ related to the integrated cross sections σ, in the electric dipole approximation, can be written[15]

$$\frac{\mathrm{d}\sigma(L_iS_i \rightarrow L_fS_f)}{\mathrm{d}\hat{k_f}} = \frac{\sigma}{4\pi}[1 + \beta P_2(\cos\theta)], \quad (2)$$

where θ are the angles between the photoelectron momentum and the incident polarization direction and $P_2(\cos(\theta))$ are the second Legendre polynomials. β, which are the asymmetry parameters defined in Ref.[15]

$$\begin{aligned}\beta(L_iS_i \rightarrow L_fS_f) =& \frac{8\pi^2\alpha a_0^2 C}{\sigma_{\mathrm{tot}}(2L_i+1)} \sum_{l_f,l_{f'}} \exp\left[-i(\sigma_{l_f} - \sigma_{l_{f'}} + \frac{i\pi}{2}(l_f - l_{f'})\right] \\ & \times ([l_f][l_{f'}])^{\frac{1}{2}} < l_f 0 l_{f'} 0 \mid 20 >< 1010 \mid 20 > \\ & \times \sum_{l_i} (-1)^{l_t}[l_t] W(1l_f 1l_{f'}; l_t 2) T^{l_t}_{L_i 1, L_f l_{f'}} (T^{l_t}_{L_i 1, L_f l_{f'}})^*, \end{aligned} \quad (3)$$

where

$$T^{l_t}_{L_i 1, L_f l_{f'}} = \sum_L (-1)^L [L]^{1/2} \left\{ \begin{array}{ccc} 1 & L_i & L \\ L_f & l_f & l_t \end{array} \right\} < \Psi_i \parallel M \parallel \Psi_f^- >,$$

$$C = \left\{ \begin{array}{ll} \omega & \text{in the length formulation} \\ \omega^{-1} & \text{in the velocity formulation} \end{array} \right.$$

$$M = \left\{ \begin{array}{ll} \sum_{j=1}^{N+1} r_j & \text{in the length formulation} \\ \sum_{j=1}^{N+1} \dfrac{\partial}{\partial r_j} & \text{in the velocity formulation} \end{array} \right.$$

with the notation $[l] = (2l+1)$. The usual notation for the C-G coefficients and 6-j symbols are applied and the σ_l in the exponential are the Coulomb phases. The requirement that the DCS in Eq.(1) should be non-negative implies that the value of the asymmetry parameters β are restricted by the inequality

$$-1 \leq \beta \leq 2. \quad (4)$$

Experimental works have provided the asymmetry parameter β_2 for the angular distribution of the total photoelectron emission to $n = 2$, which is related to β_{2s} and β_{2p} in the following way

$$\beta_2 = \frac{\sigma_{2s}\beta_{2s} + \sigma_{2p}\beta_{2p}}{\sigma_{2s} + \sigma_{2p}}. \quad (5)$$

In R-Matrix theory, it starts by partitioning configuration space into two regions by a sphere of radius a centered on the target nucleus. In inner region where $r \leq a$, electron exchange and correlation between the scattered electron and the N-electron target are important. The $(N+1)$-electron wave function in R-matrix internal region is expanded in terms of an energy-independent basis states Ψ_k. Thus,

$$\Psi_E = \sum_k C_{Ek}\Psi_k, \quad (6)$$

where the Ψ_K are given by

$$\begin{aligned}\Psi_k =& A\sum_{ij} c_{ijk}\bar{\phi}_i(x_1, ..., x_N; \hat{r}_{N+1}\sigma_{N+1}) \\ & \times \frac{1}{r_{N+1}} u_{ij}(r_{N+1}) + \sum_j \mathrm{d}_{jk}\chi_j(x_1, ..., x_{N+1}), \end{aligned} \quad (7)$$

In Eq.(7), A is the antisymmetrization operator which accounts for electron exchange between the target electrons and the free electron. The $\bar{\phi}_i$ are channel functions of the target terms that are included in the close-coupling (CC) expansion and are coupled to the angular and spin functions of the scattered electron. The χ_j in the second sum, which vanish at the surface of the internal region, are formed from the bound orbitals of $(N+1)$ system and are included to ensure completeness of the total wave function. The c_{ijk} and d_{jk} coefficients in Eq.(7) are determined by diagonalizing the (N+1)-electron Hamiltonian.

The continuum orbitals u_{ij} in Eq.(7) for each angular momentum l_i are normally obtained by solving

the model single-channel scattering problem

$$\left(\frac{\mathrm{d}^2}{\mathrm{d}r^2}-\frac{l_i(l_i+1)}{r^2}+V_0(r)+k_{ij}^2\right)u_{ij}(r) = \sum_n \Lambda_{ijn}P_{nl_i}(r), \tag{8}$$

subject to the fixed boundary conditions

$$\begin{cases} u_{ij}(0) &= 0, \\ \dfrac{a}{u_{ij}(a)}\cdot\dfrac{\mathrm{d}u_{ij}}{\mathrm{d}r}\mid_{r=a} &= 0. \end{cases} \tag{9}$$

The Lagrange multipliers Λ_{ijn} ensure that the continuum orbitals are orthogonal to bound orbitals $P_{nl_i}(r)$ of the same angular symmetry. $V_0(r)$ is a zero-order potential chosen to be the static potential of target. The k_{ij}^2 and a are the eigenvalues and the radius of the sphere defining the internal region, respectively.

The orbital functions $P_{nl}(r)$ are expressed in slater-type analytic form

$$P_{nl}(r)=\sum_{j=1}^{k}C_{jnl}\chi_{jnl}(r), \tag{10}$$

where in the Clementi-Roetti form

$$\chi_{jnl}(r)=\left[\frac{(2\xi_{jnl})^{2I_{jnl}+1}}{(2I_{jnl})!}\right]^{\frac{1}{2}}r^{I_{jnl}}\exp(-\xi_{jnl}r), \tag{11}$$

and the radial target functions satisfy the orthonormality conditions

$$\int_0^\infty P_{nl}(r)P_{n'l'}(r)\mathrm{d}r=\delta_{nn'}. \tag{12}$$

The C_{jnl}, ξ_{jnl} and I_{jnl} are Clementi-Roetti parameters[17]. In the outer region where $r \geq a$ the colliding electron is outside the atom, a set of coupled differential equations satisfied by the reduced radial wave functions are solved under infinity boundary conditions. The two regions are linked by the R-matrix on the boundary ($r = a$).[15]

R-Matrix method uses the same target orbitals in dealing with initial and final (N+1)-electron in photoionization calculations. The choice of a good basis for target states is very crucial. In the present work, the CC expansion of the He^+ target is represented by 20 states obtained from the configurations nl, $n = 1, 2, 3, 4, 5$ and $l = s, p, d, f, g$ as well as $\bar{6}s$, $\bar{6}p$, $\bar{6}d$, $\bar{6}f$, $\bar{6}g$, where $1s-5g$ are hydrogen-like wave functions of He^+. The $\bar{6}l$ are polarized correlation orbitals of the He^+ ion and represent electron correlation optimized on the ground state using the CIVPOL code.[18] In building up the set of radial functions, we have ensured that Eq.(12) is satisfied for P_{nl} with $n' \leq n$ by choosing $k = n - l$ in Eq.(10). Thus, the coefficients C_{jnl} in Eq.(10) are uniquely determined by the orthonormality conditions (12). When we fix the integers I_{jnl}, only ξ_{jnl} are treated as variational parameters. The optimized parameters are shown in Table 1. The polarized orbitals included in the target states make Eq.(7) converge faster and provide better ground state energy. Its effect on photoionization cross sections and resonance properties for He atom doubly excited states $^1P^o$ has been discussed and it well improves the agreement between the results in the length and velocity forms.[12] A severe but good test for the choice of target terms is provided by the calculation of ground state energy. The ground state of helium has an energy of $E = -4+I$ obtained from the variational principle, where I is the ionization energy. We provide an energy of -1.80243 Ry for I against the nonrelativistic limit -1.8074 Ry[19] and the calculation of -1.7908 Ry by Li and co-workers,[12] which shows it is reliable target states collected in the present work. Another good test of CI expansion is provided by the agreement of results in the length and velocity formulations, which will be discussed in the following.

Table 1. Radial function parameters for the He^+ target

orbital(nl)	C_{jnl}	I_{jnl}	ξ_{jnl}
$1s-5g$		Hydrogenlike orbitals	
$\bar{6}s$	7.39403	1	0.99478
	–14.61584	2	1.01114
	6.56315	3	0.99832
	–0.80063	4	0.99084
	0.00029	5	0.48055
	0.00001	6	0.37308
$\bar{6}p$	13.43941	2	2.22668
	–3.45470	3	1.69799
	0.00817	4	0.50277
	–0.00102	5	0.47997
	0.00003	6	0.45202
$\bar{6}d$	41.27240	3	3.69850
	–0.01845	4	1.02029
	0.00004	5	0.42455
	0.00001	6	0.41004
$\bar{6}f$	129.10304	4	4.78402
	–0.00002	5	0.57790
	0.00001	6	0.44364
$\bar{6}g$	432.73381	5	5.95148
	0.00002	6	0.43459

Ⅲ. CALCULATION AND RESULTS

The R-matrix method calculates initial bound states, excited states and final continuum states of the $(N+1)$-electron system on the same footing with the following parameters: R-matrix radius $a = 43.4\ a_0$ in Eq.(9), orbital angular moment of scattered electron $l \leq 5$ and continuum basis functions for each orbital angular momentum $N = 70$. Employing the theory described above, we have evaluated the asymmetry parameter β_2, leaving the residual He^+ ion in $n = 2$ states, and partial DCSs in $n = 2, 3, 4$ states at photon emission angle $\theta = 90°$. The results are shown in Figs. 1-5 along with available experimental data. The spectrum is dominated by resonance structures due to series of doubly-excited autoionizing states, for which the classification scheme of Herrick and Sinanoglu[20] is the most appropriate. Here the simplified nomenclature N, K_n has been used, where N and n are the principal quantum numbers of the inner and outer electron respectively, and K is the collective quantum number. The present calculations are presented with an energy mesh of $0.001-0.008$ eV, which ensure to provide all resonance states.

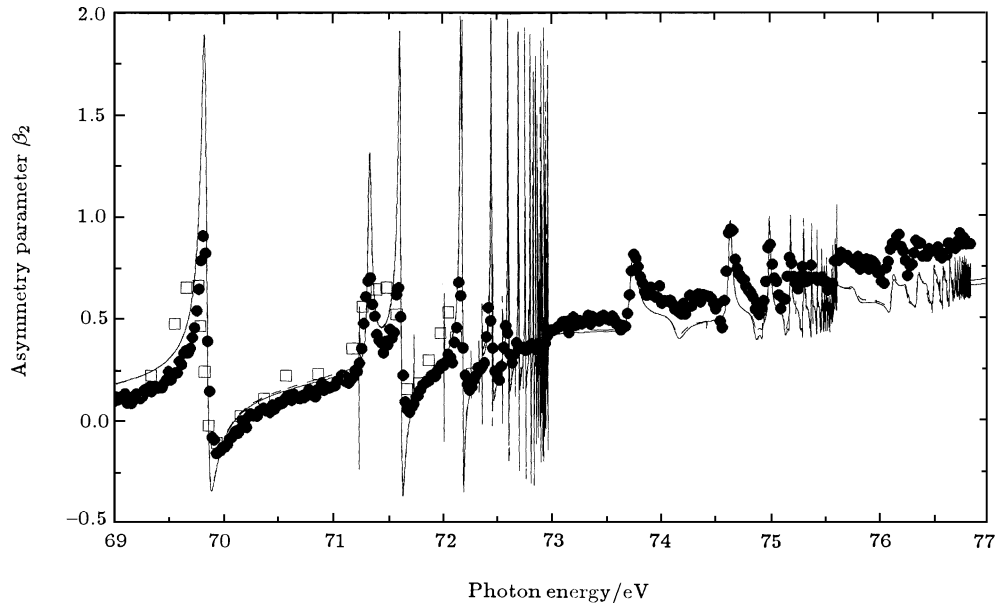


Fig.1. Asymmetry parameter β_2 in the $He^+(n = 2)$ state in the photon energy range $69-76.8$ eV. Solid line, our results in the length form; dashed line, our results in the velocity form; □, experimental data in Ref.[13]; •, experimental data in Ref.[14].

Figures 1 and 2 display our calculated asymmetry parameter β_2 and the DCS leaving He^+ ion in $n = 2$ level at $\theta = 90°$ between the $n = 2$ and $n = 5$ thresholds, respectively. The β_2 and the DCS for photoionization in the $He^+(n{=}2)$ state at $\theta = 90°$ have been obtained in experiments as a continuous function of photon energy by Zubek *et al.*[14] with linearly polarized light and they are also shown in Figs.1 and 2 for comparison with present calculations. In Fig.1, the experimental results of Lindle *et al.*[13] are also plotted in the region below 73 eV. At first, good agreement between our calculations in the length and velocity forms is shown in the figure. Comparison with two experimental measurements is good in general, particularly below the $n{=}3$ threshold. Between the thresholds of $n{=}2$ and $n{=}3$(about $69-73$ eV), Sanchez and Martin[7] in 1992 reported their theoretical calculations on the β_2 for photoionization (Fig. 4 in Ref.[7]) based on Feshbach partitioning of the final-state wave function and an L^2 representation of the coupled continuum states. Since we cannot collect their exact theoretical data, a direct comparison between the two approaches is not given in present work. However, we may learn from Fig.4 in Ref.[7] that their calculations on the qualitative cure shapes and the positions of resonance states agree well with ours and experimental data. The difference in the two theoretical results is that the magnitude of the peaks in the calculations of Sanchez and Martin[7] are lower than the present calculations and two available experimental data. Though they are in good agreement in the positions and shapes of resonance states, the present re-

sults present a magnitude smaller compared with the measurements of Zubek *et al.*[14] in the region of above the n=4 threshold. No other theoretical and experimental β_2 results are found up to now in the region. In addition, the experimental resolution is responsible for the absence of some needlelike peaks in both experiments. Therefore, the present resonant structures are much richer in the β_2 parameter.

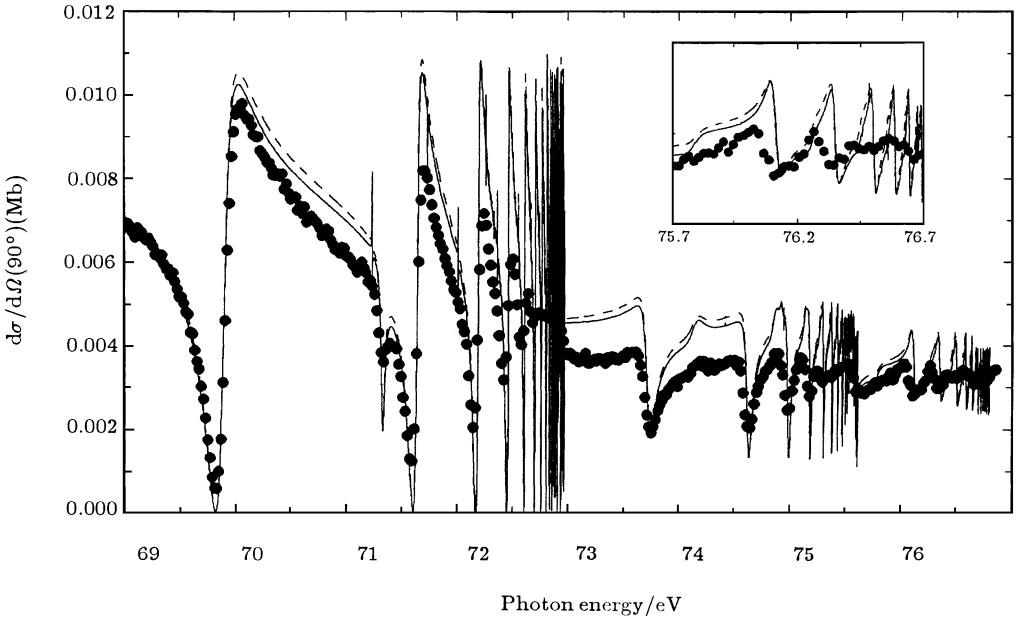


Fig.2. Differential cross section for photoionization into the $He^+(n = 2)$ state at $\theta = 90°$ in the photon energy range $69 - 76.8$ eV. Solid line, our results in the length form; dashed line, our results in the velocity form; •, experimental data in Ref.[14].

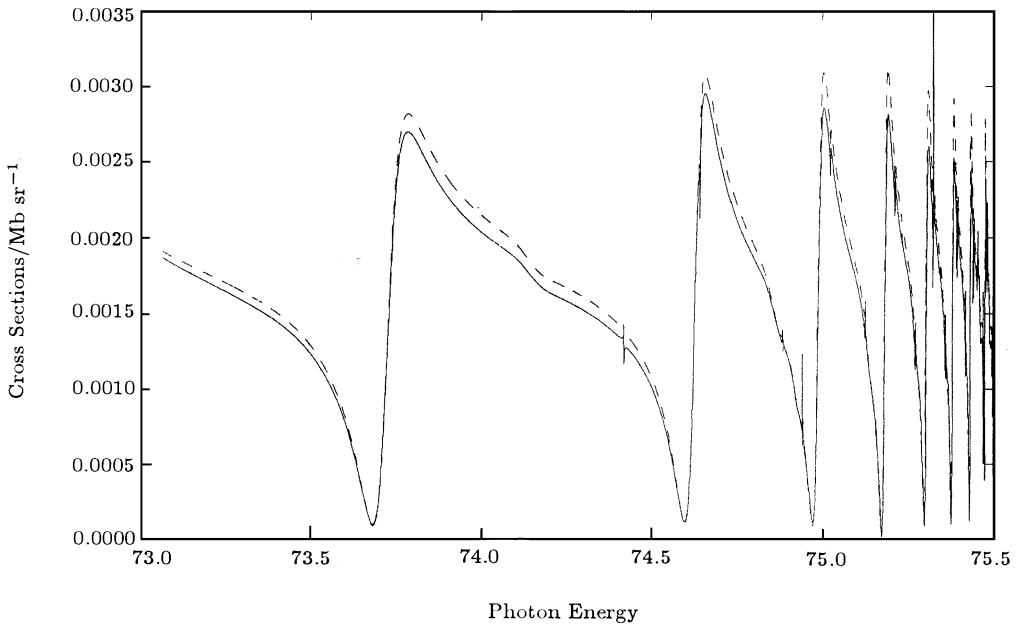


Fig.3. Differential cross section for photoionization into the $He^+(n = 3)$ state for $\theta = 90°$ at $73 - 75.5$ eV. Solid line, our results in the length form; Dashed line, our results in the velocity form.

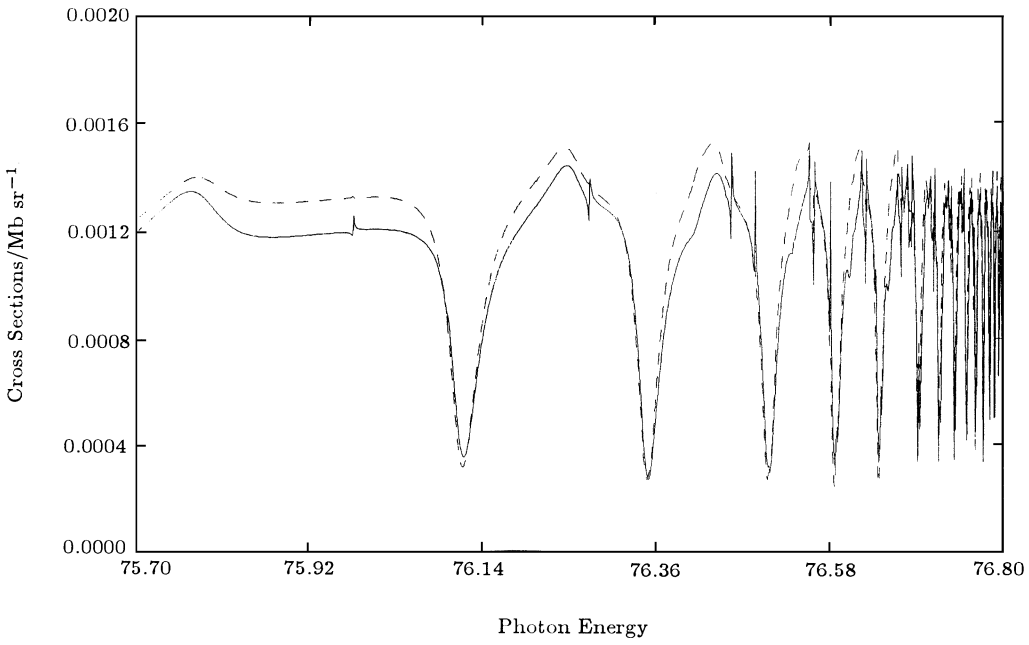


Fig.4. Same as figure 3 but for photoionization cross section into the $He^+(n = 3)$ state for $\theta = 90°$ at $75.7 - 76.8$ eV.

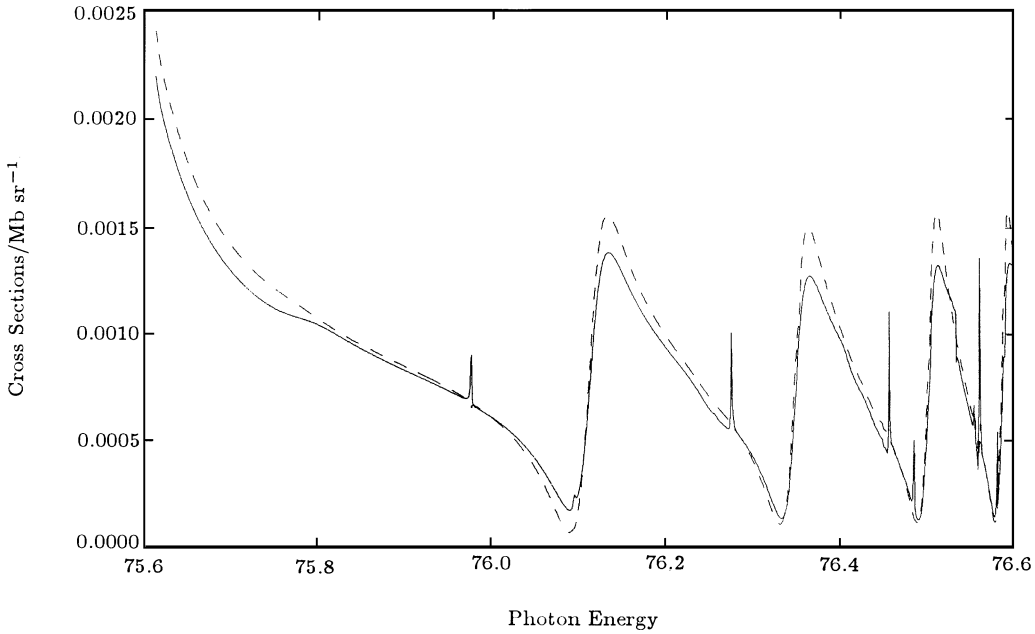


Fig.5. Same as figure 3 but for photoionization cross section into the $He^+(n = 4)$ state for $\theta = 90°$ at $75.6 - 76.6$ eV.

In Fig.2, good agreement in the length and velocity forms means that the target functions collected are reliable. In general, the present DCS of photoionization into $He^+(n{=}2)$ is in fairly good agreement in the positions and shapes of observable[14] and calculated[7] autoionization resonance states at present photon energies concerned. However, the difference has been found that their positrons of $3, 1_n$ states in Fig.6 in Ref.7 shift to higher energies compared with the measurements of Zubek *et al.* and the present calculations. Between the $n{=}2$ and $n{=}3$ thresholds, the spectrum includes five series of resonance which are, in the independent-electron limit, correlated to configurations of the forms $3sn'p'$, $3pn's'$, $3pn'd'$, $3dn'p'$, $3dn'f'$. The lowest member of much weaker $3, 1_n$ series can also be seen clearly in Zubek's measurements and has a good agreement against the two theoretical values. In addition, present theoretical results

give some high-lying resonance states $3,1_n$ $n \geq 7$ and they are not provided in experiments due to lower resolution of 60 meV. The very narrow 2_n resonance states are seen clearly in the present work from Fig.1, and due to the lower energy resolution of the photoelectron (60 meV), this resonance series was not observed in experiments of Zubek et al. Between the n=3 and n=5 thresholds(about at $73 - 76.8$ eV), no other calculations on the DCS of photoionization into $He^+(n=2)$ at 90° are found until now in the literature. Figure 2 shows that present calculations reproduce strong series corresponding to the $4,2_n$ and $5,3_n$ converging to the $He^+(n=4)$ and $He^+(n=5)$ ionization thresholds against experiments, respectively. The $4,0_4$(about at 74.12 eV) state observed in experiments is also provided in present results and good agreement in positron and shape is obtained in Fig 2. Apart from that, the present calculations on DCS for photoionization provide much richer resonance structures than the available experimental measurements due to the lower resolution.

Figures 3 and 4 give the DCS for photoionization leaving He^+ ion in n=3 state in different photon energy region and Fig.5 is for the results in n=4 state. Good agreement in present length and velocity formulations is also shown in the figures, and no other available theoretical and experimental data are found until now. Present results provide rich resonance series and it is difficult to identify them correctly. However, Comparing Figs.2–5, we found the resonance features, which can be seen in these spectra, have of course the same origin, but the line shapes and relative strengths are seen to depend strongly on the final states($n = 2, 3$ or $n = 4$). For the same resonance series, their magnitude for photoionization into $He^+(n = 2)$ is higher than those to $He^+(n = 3)$ and $He^+(n = 4)$. As seen in Figs.2–5, the magnitude of resonance state depends strongly on He^+ ion states, and the magnitude decreases as the states of He^+ ion are varied from $n = 2$ to 3 and 4. In addition, some series such as $5,1_n$, can be shown more clearly in spectra into $n = 3$ and $n = 4$(Figs.4 and 5) states than that into $n = 2$ state above 75.7 eV. In addition, we also notice that the shapes on some resonances series are different according to different He^+ ion $n = 2, 3, 4$ states such as the resonance state occurring at about 76.27 eV in Figs.4 and 5. On the other hand, some differences in magnitude also lie in our results in the length and velocity forms in Figs.1−5. This is because the target functions and continuum orbitals included in the present approach are not too much according to the limit of our present computer condition. In addition, the spectrum becomes very complex due to the strong interchannel interference, resulting from nine correlated configurations between the $n = 4$ and $n = 5$ thresholds. Thus, it is difficult to calculate the photoionization spectra at higher photon energies due to multitudes of resonances and perturbation by next series(above the $n = 5$ threshold), particularly in the β_2 and the DCS for photoionization.

IV.CONCLUSIONS

We have calculated the asymmetry parameter β_2 leaving the He^+ ion in the n=2 level, and the partial differential cross sections for photoionization from the ground state $^1S^e$ to final state $^1P^o$ leaving He^+ ion n=2, 3, 4 at $\theta = 90°$ between the n=2 and n=5 thresholds employing R-matrix method with a 20-term target representation. The quality of the target wave functions as well as bound and continuum ones for e+He^+ system is proved when comparing the ionization energy I of He atom and the agreement of results in the length and velocity forms. Our results are compared with the available theoretical and experimental results and good agreements are obtained. Between the n=3 and n=5 thresholds, we firstly present theoretical values of the asymmetry parameter β_2 and the partial DCSs for photoionization leaving He^+ ion in $n = 2, 3, 4$ levels at photon emission angle $\theta = 90°$; and no comparable measurements and calculations for the DCSs into He^+ ion n=3,4 states at $\theta = 90°$ are available. Here, we notice that the present calculations provide rich resonance states on the β_2 and the DCSs for photoionization into $He^+(n = 2, 3, 4)$ states. Thus, we hope to have more experimental work with higher energy resolution and theoretical researches to check the present data of β_2 and DCS for photoionization, particularly between the $n = 3$ and $n = 5$ thresholds region.

ACKNOWLEDGEMENT

The present work was completed in Tsinghua University and the authors would like to thank Prof. Jiaming Li and Dr. Jun Yan, Tsinghua University, for their suggestions and help.

REFERENCES

[1] D. W. Lindle, T. A. Ferrett, P. A. Heimann and D. A. Shirley, *Phys. Rev.,* **A36**(1987),2112.

[2] M. Domke, G. Remmers and G. Kaindl, *Phys. Rev. Lett.,* **69**(1992),1171.

[3] M. Domke, K. Schulz, G. Remmers and G. Kaindl, *Phys. Rev.,* **A53**(1996),1424.

[4] K. Schulz, G. Kaindl, M. Domke, J. D. Bozek, P. A. Heimann, A. S. Schlachter and J. M. Rost, *Phys. Rev. Lett.,* **77**(1996),3086.

[5] D. R. Herrick and O. Sinanoglu, *Phys. Rev.,* **A11**(1975), 97.

[6] R. Moccia and P. Spizzo, *J. Phys.,* **B20**(1987),1423; *Phys. Rev.,* **A43**(1991),2199.

[7] I. Sánchez and F. Martín, *Phys. Rev.,* **A45**(1992),4468.

[8] J. Z. Tang, S. Watanable and M. Matsuzawa, *Phys. Rev.,* **A48**(1993),84; *Phys. Rev. Lett.,* **69**(1992),1633.

[9] T. N. Chang, *Phys. Rev.,* **A47**(1993),3441; **47**(1993),705.

[10] B. Zhou and C. D. Lin, *J. Phys.,* **B26**(1993),2575.

[11] T. W. Gorczyca and N. R. Badnell, *J. Phys.,* **B30** (1993),3897.

[12] J. Yan, Y. Z. Qu, Lan Vo ky and J. M. Li, *Phys. Rev.,* **A57**(1998),997.

[13] D. W. Lindle, T. A. Ferrett, U. Becker, P. H. Kobrin, H. G. Kerkhoff and D. A. Shirley, *Phys. Rev.,* **A31**(1985),714.

[14] M. Zubek, G. Dawber, R. I. Hall, L. Araldi, K. Ellis and G. C. King, *J. Phys.,* **B24**(1991),L337.

[15] P. G. Burke, A. Hibbert and W. D. Robb, *J. Phys.,* **B4**(1971),153.

[16] K. A. Berrington, P. G. Burke, K. Butler, M. J. Seaton, P. J. Storey, K. T. Taylor and Y. Yu, *J. Phys.,* **B20**(1987),6379.

[17] E. Clementi and R. Roetti, *At. data Nucl. Sata Tables* **14**(1974),177.

[18] M. Le Dourneuf(unpublished); Vo ky Lan, M. Le Dourneuf and P. G. Burke, *J. Phys.,* **B9**(1976),1065.

[19] C. L. Pekeris, *Phys. Rev.,* **162**(1962),1470.

[20] D. R. Herrick and O. Sinanoglu, *Phys. Rev.,* **A11**(1975), 97.